Iranian Polymer Journal
20 (9), 2011, 735-746

Available online at: http://journal.ippi.ac.ir

Prediction of Fracture Toughness for Open Cell Polyurethane Foams By Finite-element Micromechanical Analysis

Emanoil Linul and Liviu Marsavina*

Strength of Materials Department, Polytechnic University of Timisoara, Timisoara-300222, Romania

Received 9 April 2011; accepted 17 August 2011

A B S T R A C T

The fracture toughness was determined for cellular polymers by micromechanical modelling using finite element analysis. In this study, mode I and mode II of fracture toughness were evaluated with a 2D-solid model using fracture analysis code FRANC2D/L. Simulation was performed for open cell polyurethane foams of different densities. Two cases were considered: constant cell length, l, and variable cell wall thickness; the former for constant cell wall thickness, t, and the latter for variable cell length. For estimation of fracture toughness the applied loads were progressively increased to the point reaching the fracture strength of the solid material (130 MPa) in an un-cracked strut in front of the crack. The estimated fracture toughness was independent on crack length, indicating that the obtained values could be considered as material property. The values of the fracture toughness of polyurethane foams are in the range of 10^{-3}-10^{-1} MPa.$m^{0.5}$. Lower values were obtained for mode II fracture toughness. A strong dependency of the fracture toughness on the density of the cellular material was featured by present study. The obtained results for mode I fracture toughness were compared with Gibson-Ashby micromechanical model, by which a good agreement was obtained. While, mode II fracture toughness was compared with Choi and Sankar micromechanical models. The predicted fracture toughness was finally validated with some experimental data. Another advantage of this model was to obtain a fully described the stress field in the solid struts. The stress distribution in the first un-cracked strut showed a combined stress (bending and tension) for mode I loading, while for mode II loading a pure bending appeared.

Key Words:

polyurethane foam;
open cell;
fracture toughness;
finite element analysis;
micromechanical model.

INTRODUCTION

Cellular materials are composed of an interconnected network of solid layers with shaped edges and well-defined faces [1]. Given the properties of solid materials and the geometry of cell structure, an important objective is to estimate the properties of cellular material. Such properties are sometimes difficult to be determined experimentally, but they are necessary for design purposes [2]. Network-type models are often used as micromechanical tools. The cellular material shows an anisotropic structure and micromechanical models which may be taken into account for properties and response [3-6]. Finite element modelling methods are used to describe the behaviour and the mechanical properties of cellular structures [7]. The analytical micromechanical models could be also considered

(*) To whom correspondence to be addressed.
E-mail: msvina@mec.upt.ro

[1,8]. The micromechanical analyses assess locally the stress and the displacement fields. These microstructures related details are particularly important to understand and describe the deterioration and fracture of the cellular materials [9-11].

Detailed studies on the micromechanical models for cellular materials are presented by Gibson et al. [1] and Mills [12], who focus only on micromechanical models related to fracture toughness. The micromechanical models relate the fracture toughness of rigid foams, K_{IC}, to the struts solid material fracture strength, σ_{fs}, relative density, ρ^*/ρ_s, and geometric characteristics of open-cell cellular materials (the cell length, l, and strut thickness, t, as depicted in Figure 1). Gibson and Ashby considered that, at the cells' scale, a crack can be extended in a discrete mode [1]. The model is based on a 2D honeycombs and every time the row of cells breaks along the crack front, the crack extends with the cell length (Figure 2). If the foam is loaded, the walls of the cell deform elastically. The load is transmitted through the foam as a discrete set of forces and moments through cells edges. These forces and moments can be calculated based on linear elastic stress field in the vicinity of the crack. Gibson and Ashby assumed that the tip of the crack is located half way the length of the edge and the applied load corresponds to mode I [1]. They considered that the first unbroken strut is subject only to bending, while in reality an important tensile load is also present. Comparing with experimental data for different cellular materials with open-cells: Fowlkes for polyurethane [13], McIntyre et al. for polyurethane [14], Maiti et al. for PMMA [15], Brezny et al. for ceramic foams [16], conclude the relationship between fracture toughness and relative density in the form:

$$\frac{K_{IC}}{\sigma_{fs}\sqrt{\pi l}} = 0.65\left(\frac{\rho^*}{\rho_s}\right)^{1.5} \quad (1)$$

It should be mentioned that Gibson and Ashby did not predict the value 0.65, but only the slope 1.5 of the

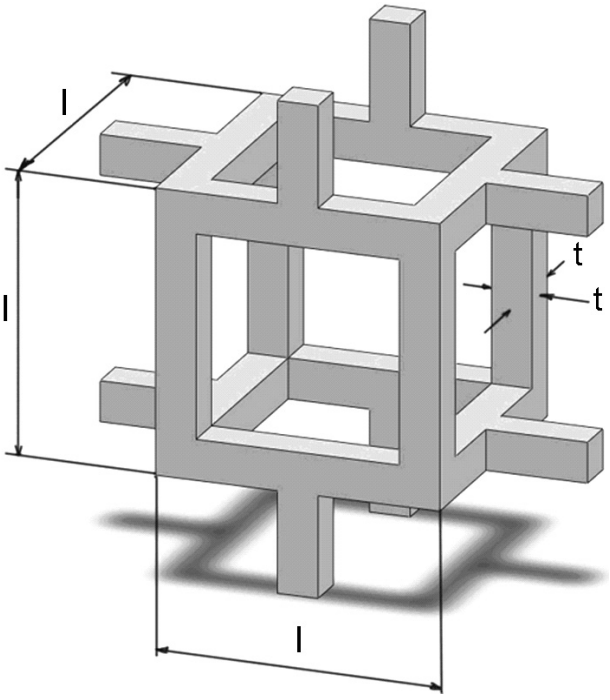

Figure 1. A cubic model for an open-cell foam with the edge length, l and the edge thickness, t [1].

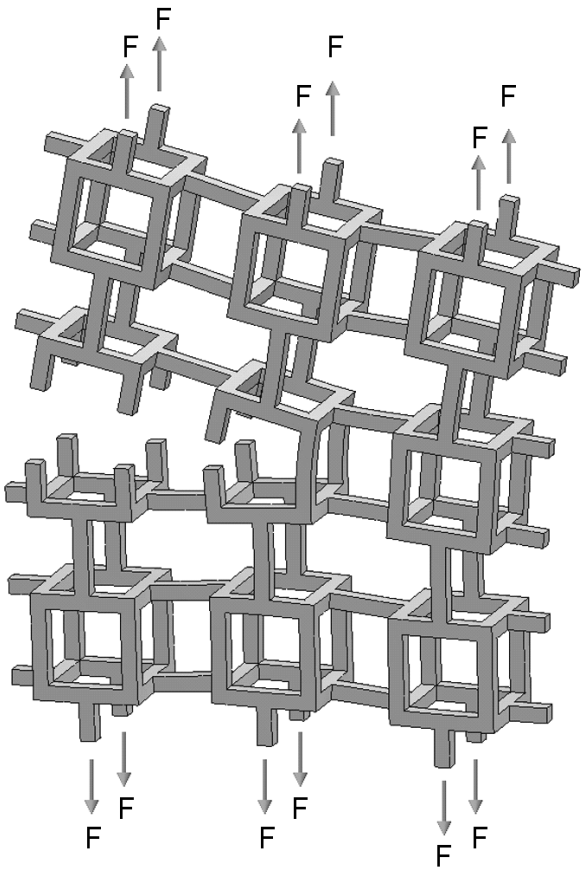

Figure 2. Propagation of a crack through brittle open-cell foam [1].

power law relationship. They plotted experimental data and inferred that the constant for real foams might be 0.65. The experimental results on carbon foams [17] show that only for a/l>10, eqn (1) is consistent with the crack length, a. A similar relation was proposed by Green, considering the elastic deformation shell theory of hollow sphere model for foam cells [18]. Another model was proposed by Choi et al., taking into account that, due to crack blunting, the stress field around the crack in the foam is non-singular [19]. Choi et al. [20] proposed another micromechanical model, considering for mode I that bending and tensile occur in the first strut in front of the crack, while for mode II the shear force was involved. They proposed the semi-empirical expressions for fracture toughness, depending on tensile strength of solid material, cell dimensions (length and thickness) and crack length.

In recent years, finite element analysis (FEA) is used extensively in order to solve the micro-mechanical models for fracture toughness estimation of cellular materials. Choi et al. [20] proposed a beam finite elements model and investigated mode I (Figure 3), mode II (Figure 4) and mixed loading modes. The fracture toughness of carbon foam was related to relative density for two considered cases: constant cell length and constant strut thickness. The obtained expressions of fracture toughness could be summarized as follows:

- For constant cell length, l = 200 μm:

$$K_{IC} = 1.961\left(\frac{\rho^*}{\rho_s}\right)^{1.045}$$

and

$$K_{IIC} = 6.95\left(\frac{\rho^*}{\rho_s}\right)^{1.32} \quad (2)$$

- For constant strut thickness, t = 20 μm:

$$K_{IC} = 7.82\left(\frac{\rho^*}{\rho_s}\right)^{0.788}$$

and

$$K_{IIC} = 2.76\left(\frac{\rho^*}{\rho_s}\right)^{1.07} \quad (3)$$

Ableidinger [21] investigated a compact tension specimen, made of open cell aluminium foam subject to monotonic loading. The region surrounding the crack tip was modelled with a fully three-dimensional tetrakaidecahedral open cell micro-geometry, meshed with beam elements. Arakere et al. [22] used a 3D model for the determination of fracture toughness for BX-265 foam (density: 32.5 kg/m^3), an isolation material used for external shuttle tank. Material was

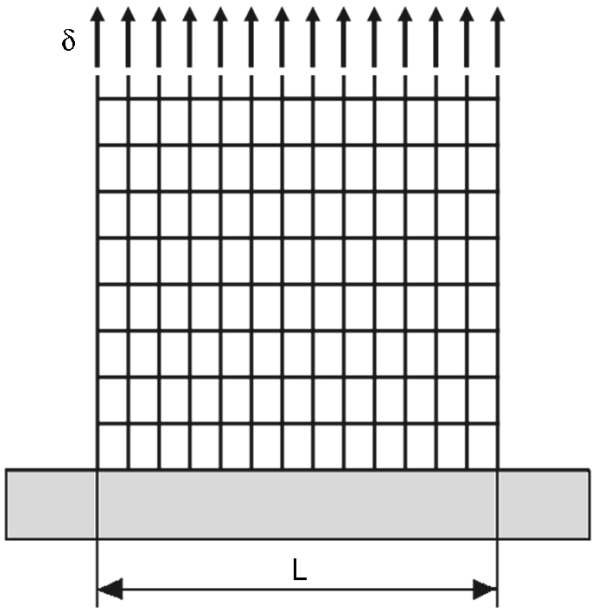

Figure 3. Beam finite element model for mode I [20].

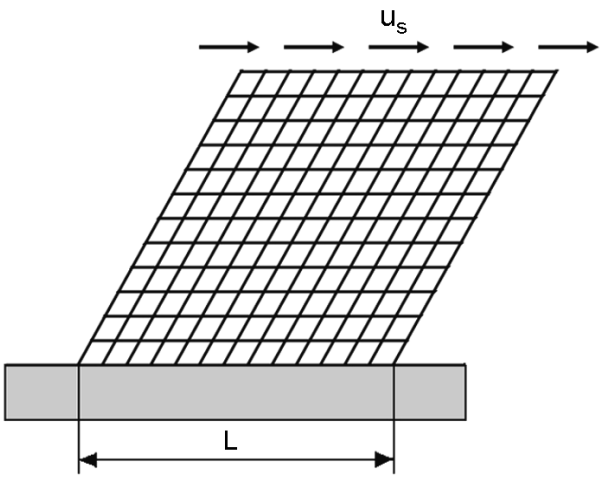

Figure 4. Beam finite element model for mode II [20].

considered as an anisotropic solid and the stress and fracture analyses included the effect of direction dependence on material properties (transversally isotropic material results after experimental tests). Middle tension specimens were considered and M-Integral method was applied for determining the stress intensity factors.

A 3D-solid model was proposed by Choi et al. [23] in order to find the mode I fracture toughness of carbon foam. The micromechanical-based fracture toughness results were compared with the experimental tests, based on singular edge notched specimens, and good agreement was obtained.

All micromechanical models described above relate the fracture toughness of foams with the fracture strength of solid material, cell length and relative density. Their advantages and disadvantages are discussed in Marsavina [24]. However, the mode II fracture toughness was presented only by Choi et al. [20] and was based on a beam finite element model.

This paper proposes a new solid finite element model, based on rectangular cell geometry, for estimation of mode I and mode II of fracture toughness of polyurethane foams. The main advantage of this model is the possibility to represent the stress field around cracks in cellular materials. The presence of tensile, together with bending, in the first unbroken strut under mode I loading is highlighted by the numerical results. A convergence study was performed in order to choose the optimum size of the finite element model. The influence of the crack length on the fracture toughness results is also investigated and it appears to have no influence on the estimated fracture toughness. The obtained results for polyurethane fracture toughness are finally compared with other micromechanical models proposed in literature and with some experimental fracture toughness data [4,25,26].

Finite Element Micromechanical Model for Fracture Toughness Determination

The properties of foams depend on the geometrical characteristics of cells and, as a consequence, on the relative density. For open foams with strut length, l, and strut thickness, t, the relative density is given by [1]:

$$\frac{\rho^*}{\rho_s} = 2\frac{t}{l}\left(1-\frac{1}{2}\frac{t}{l}\right) \quad (4)$$

If the strut thickness, t, is much smaller than l, the strut length (t << l), we can use a simplified relation between relative density and strut length and thickness [1]:

$$\frac{\rho^*}{\rho_s} = 2\frac{t}{l} \quad (5)$$

The finite element study investigates the influence of cell dimensions and relative density on the fracture toughness of open cell polyurethane foams.

Finite Element Model

The paper presents a micromechanical model for the prediction of fracture toughness for cellular materials, using finite element analysis and fracture analysis code FRANC2D/L. The finite element model is similar to the Huang and Gibson 2D-solid cubic model [17]. In comparison with the Choi et al. [20] 2D models, where beams were considered as foam struts, the geometry of solid struts is modelled in the proposed 2D-solid model.

The polyurethane foams are orthotropic at macroscale, due to the manufacturing process, resulting in different cell sizes in-plane and out-of-plane. For this attempt, we have considered, at cell level that the behaviour is isotropic by using constant cell dimensions.

Simulation was performed for open cell polyurethane foams, considering the following cases:

- Quasi-constant cell length, l = 0.52-0.60 mm, and variable strut thickness (0.1, 0.05 and 0.02 mm),
- Constant strut thickness, t = 0.05 mm, and variable cell length (0.55, 0.75 and 0.95 mm).

The mechanical characteristics of the solid polyurethane material considered in the simulation were: density, ρ = 1170 MPa, fracture strength, σ_{fs} = 130 MPa, Young's modulus, E = 1600 MPa, and Poisson's ratio, ν = 0.4.

Both fracture modes I and II were considered. The plane strain micromechanical model used for mode I is shown in Figure 5a, and Figure 5b presents the model for mode II, representing a quarter from a central cracked foam. The boundary conditions are

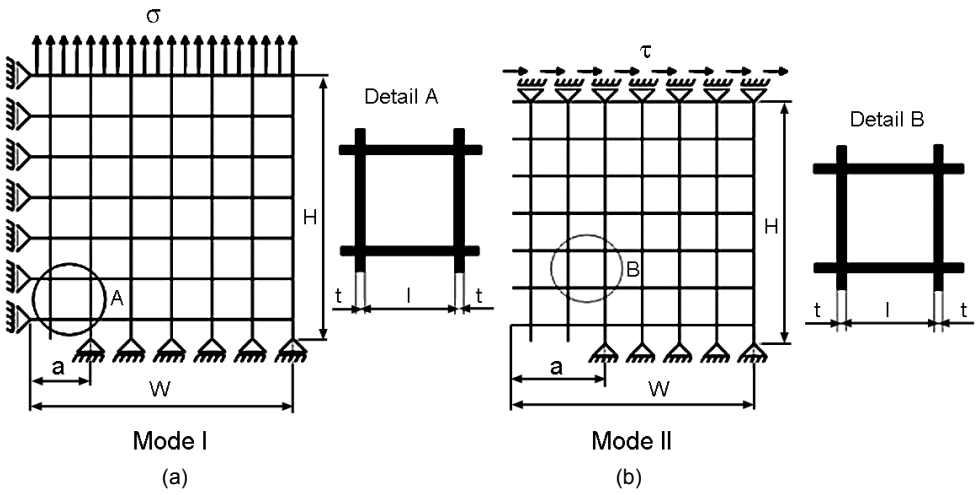

Figure 5. Micromechanical model dimensions and boundary conditions: (a) mode I and (b) mode II.

also shown in Figure 5. In order to obtain the fracture toughness, the models were loaded progressively, with σ for mode I and with τ for mode II, respectively. The fracture toughness for both K_{IC} and K_{IIC}, were obtained equating with the stress intensity factors solutions provided in Murakami (Scheme I) [27], where a (mm) is the crack length, W (mm) is the width of the model, respectively σ, and τ values of the applied load for which the maximum stress, $\sigma_{y,max}$, in the first un-cracked strut reaches the fracture strength of the solid material, σ_{fs}.

A total number of 276 models were analyzed. The characteristics of numerical models are presented in Table 1: the number of elements (plane 8 nodes quadratic elements) and nodes.

Convergence Study and Influence of Crack Length

A convergence study was carried out on the micro-mechanical models composed from 4×4 cells to 10×10 cells. The results for mode I and mode II of fracture toughness of PUR foam with relative density of 0.105 versus the number of cells are plotted in Figure 6a. The relative difference between the minimum and the maximum values in fracture toughness is 14.3% for mode I and 7.9% for mode II. This difference decreases, for models with 64 cells and 100 cells, to 5.4% for mode I and to 3.3% for mode II. However, the influence in computational time between models with 64 and 100 cells is insignificant and the 100 cells model was used for fracture toughness assessment.

Figure 6b presents the influence of crack length on fracture toughness for PUR foam with relative density of 0.105. Six different crack lengths were considered as 1.4, 2.35, 3.3, 4.25, 5.2 and 6.15 mm, keeping the size of the foam constant. The relative

$$K_I = \sigma\sqrt{\pi a}\, F_I(a/W) = K_{IC}$$
$$K_{II} = \tau\sqrt{\pi a}\, F_{II}(a/W) = K_{IIC} \quad (6)$$

$$F_I(a/W) = \frac{1-0.5(a/W)+0.37(a/W)^2-0.044(a/W)^3}{\sqrt{1-a/W}} \quad (7)$$
$$F_{II}(a/W) = 1.50+0.569(a/W)-6.282(a/W)^2-38.157(a/W)^3+21.01(a/W)^4$$

Scheme I

Table 1. Model dimensions.

Model (t×l) (mm)	Relative density	Number of cells	Model dimension		Number of elements	Number of nodes
			W = H (mm)	a (mm)		
0.1×0.6	0.333	16	2.15	0.85; 1.45	624	2456
		25	2.75	0.85; 1.45; 2.05	1000	3925
		36	3.35	0.85; 1.45; 2.05	1464	5736
		49	3.95	0.85; 1.45; 2.05; 2.65	2016	7889
		64	4.55	0.85; 1.45; 2.05; 2.65; 3.25	2656	10384
		81	5.15	0.85; 1.45; 2.05; 2.65; 3.25; 3.85	3384	13221
		100	5.75	0.85; 1.45; 2.05; 2.65; 3.25; 3.85	4200	16400
0.05×0.55	0.182	16	1.95	0.8; 1.35	624	2456
		25	2.50	0.8; 1.35; 1.9	1000	3925
		36	3.05	0.8; 1.35; 1.9	1464	5736
		49	3.60	0.8; 1.35; 1.9; 2.45	2016	7889
		64	4.15	0.8; 1.35; 1.9; 2.45; 3	2656	10384
		81	4.70	0.8; 1.35; 1.9; 2.45; 3; 3.55	3384	13221
		100	5.25	0.8; 1.35; 1.9; 2.45; 3; 3.55	4200	16400
0.02×0.52	0.077	16	1.86	0.77; 1.29	2864	11416
		25	2.35	0.77; 1.29; 1.81	4600	18325
		36	2.87	0.77; 1.29; 1.81	6744	26856
		49	3.39	0.77; 1.29; 1.81; 2.33	9296	37009
		64	3.91	0.77; 1.29; 1.81; 2.33; 2.85	12256	48784
		81	4.43	0.77; 1.29; 1.81; 2.33; 2.85; 3.37	15624	62181
		100	4.95	0.77; 1.29; 1.81; 2.33; 2.85; 3.37	19400	77200
0.05×0.75	0.133	16	2.65	1.1; 1.85	1632	6488
		25	3.40	1.1; 1.85; 2.6	2620	10405
		36	4.15	1.1; 1.85; 2.6	3840	15240
		49	4.90	1.1; 1.85; 2.6; 3.35	5292	20993
		64	5.65	1.1; 1.85; 2.6; 3.35; 4.1	6976	27664
		81	6.40	1.1; 1.85; 2.6; 3.35; 4.1; 4.85	8892	35253
		100	7.15	1.1; 1.85; 2.6; 3.35; 4.1; 4.85	11040	43760
0.05×0.95	0.105	16	3.35	1.4; 2.35	2080	8280
		25	4.30	1.4; 2.35; 3.3	3340	13285
		36	5.25	1.4; 2.35; 3.3	4896	19464
		49	6.20	1.4; 2.35; 3.3; 4.25	6748	26817
		64	7.15	1.4; 2.35; 3.3; 4.25; 5.2	8896	35344
		81	8.10	1.4; 2.35; 3.3; 4.25; 5.2; 6.15	11340	45045
		100	9.05	1.4; 2.35; 3.3; 4.25; 5.2; 6.15	14080	55920

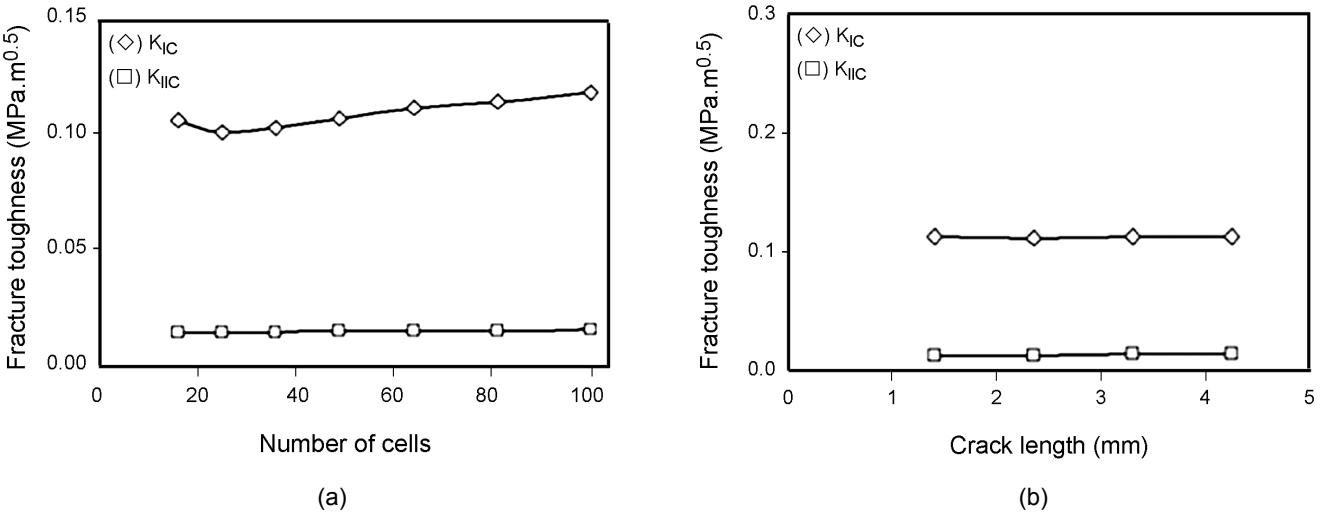

Figure 6. Influence of cell number and crack length in fracture toughness: (a) variation of fracture toughness with number of cells and (b) variation of fracture toughness with crack length.

differences in fracture toughness were 1.3% for mode I and 4.3% for mode II, indicating that the predicted fracture toughness could be considered independent on crack length.

Figure 7 presents the deformed mesh for crack length, a = 0.85 mm, and different numbers of cells (from 16 to 100 cells) loaded in mode I.

Mode I Fracture Toughness

The crack is assumed to be normal to the loading direction. The crack is created by breaking the ligaments of the cells [23]. Figure 8 shows the deformed mesh for rigid polyurethane foam with l = 0.6 mm and t = 0.1 mm, with different crack lengths.

Mode I fracture toughness was obtained by progressively increasing the applied load, σ, until the maximum load in the first unbroken strut reached the fracture strength of the solid, σ_{fs}, as indicated in Figure 9b. This value of the applied load, σ, was used in eqn (6) to predict the fracture toughness, K_{IC}. A combined stress (tensile with bending) occurs in the first strut, Figure 9, which confirms the hypothesis

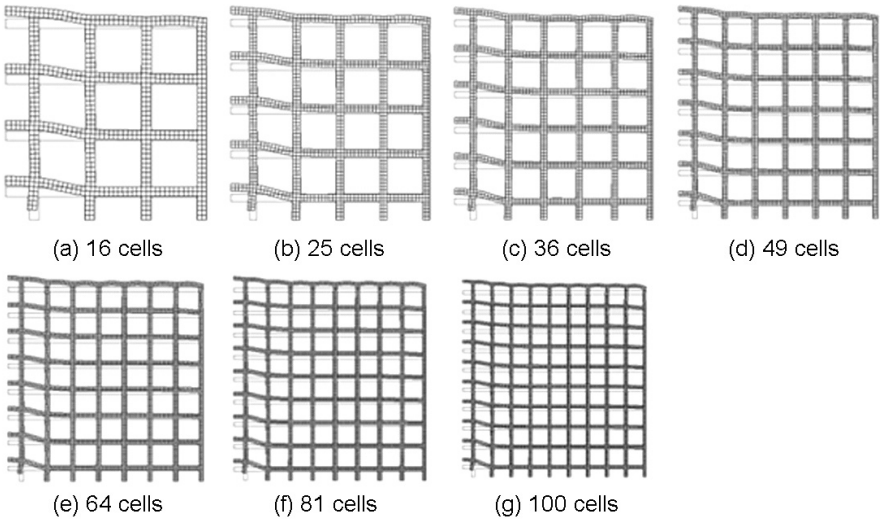

Figure 7. Deformed meshes for crack length, a = 0.85 mm, loaded in mode I with different number of cells.

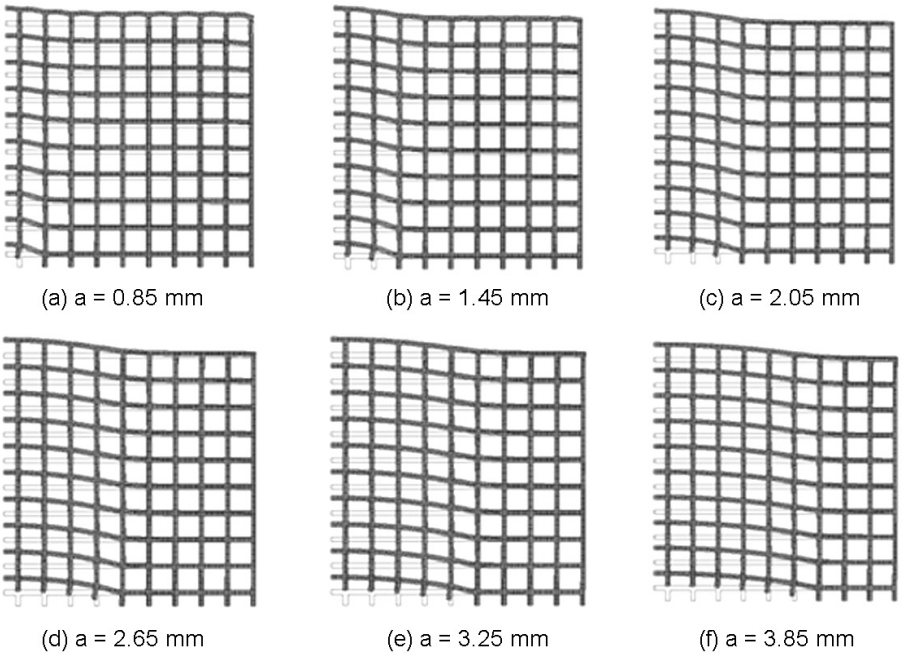

Figure 8. Deformed meshes for different mode I loading: (a) a = 0.85 mm, (b) a = 1.45 mm, (c) a = 2.05 mm, (d) a = 2.65 mm, (e) a = 3.25 mm and (f) a = 3.85 mm.

underlying the micromechanical model of Choi et al. [20], and disagrees the hypothesis proposed by Gibson et al. [1] which takes into account only the bending stress.

Variation of mode I fracture toughness versus relative density for rigid polyurethane foam is shown in Figure 10. Fracture toughness values ranging between 0.051 MPa.m$^{0.5}$, for relative density of 0.077, up to 0.384 MPa.m$^{0.5}$, for relative density of 0.333, were obtained. It can be observed in Figure 10 that the relative density created by either constant length or constant strut thickness causes different variations on the obtained fracture toughness. This could be explained by eqn (5) in which the relative density is directly proportional with strut thickness, t, and inversely proportional with strut length, l.

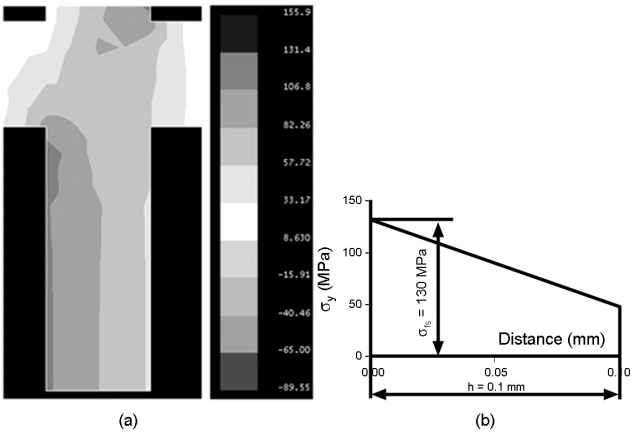

Figure 9. Stress distribution, σ_y, in first unbroken strut for mode I loading: (a) contour plot and (b) line plot.

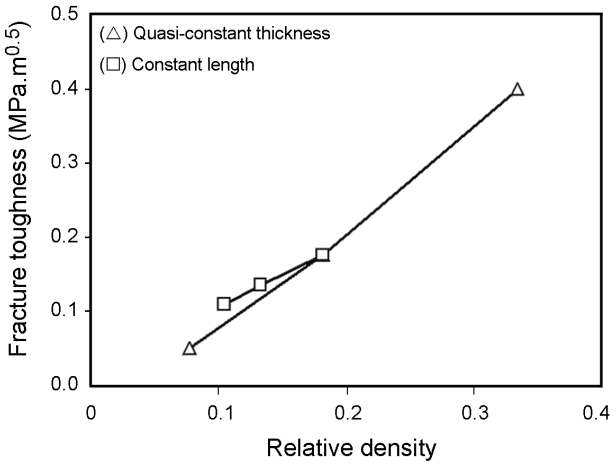

Figure 10. Mode I fracture toughness as a function of relative density for two considered cases: constant cell length and constant strut thickness.

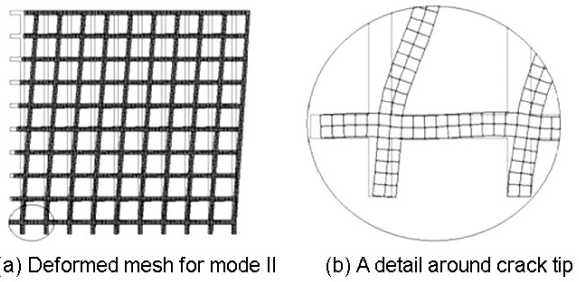

Figure 11. Deformation of the foam subjected to mode II loading for a = 0.85 mm.

Mode II Fracture Toughness

Analysis for mode II fracture toughness is similar to that described for mode I. An example of deformed mesh in mode II, for a foam with l = 0.55 mm and t = 0.05 mm, is shown in Figures 11a and 11b which present the details of the cracked area.

The stress distribution, σ_y, in the first unbroken strut can be observed in Figure 12a, and the variation of stress on the strut thickness is presented in Figure 12b. Pure bending appears in the strut with the maximum tensile stress near the crack tip. The value of the applied load, τ, which produced the stress, $\sigma_{y,max} = \sigma_{fs}$, was used in eqn (6) for estimating the fracture toughness.

Figure 13 shows the fracture toughness of rigid polyurethane foam versus relative density for mode II. Mode II fracture toughness values range between 0.006 MPa.m$^{0.5}$, for relative foam density of 0.077, and 0.105 MPa.m$^{0.5}$, for relative density of 0.333.

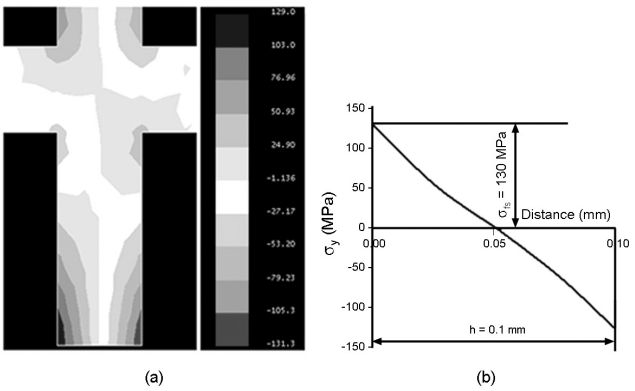

Figure 12. Stress distribution, σ_y, in first unbroken strut for mode II loading: (a) contour plot and (b) stress distribution on strut thickness.

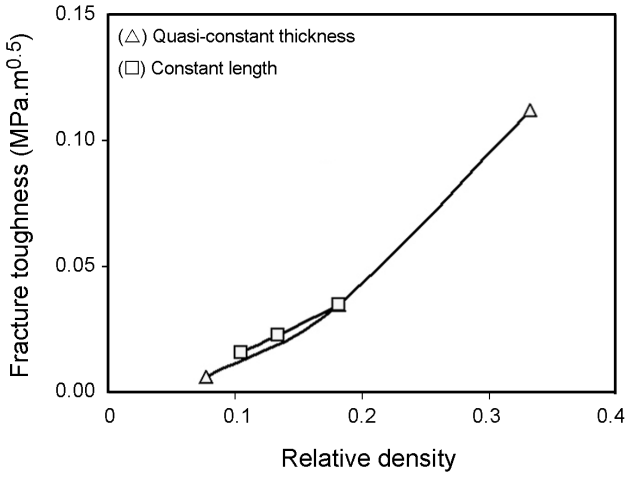

Figure 13. Mode II fracture toughness as a function of relative density for the two cases: constant length (0.5 mm) and constant strut thickness (0.05 mm).

Comparison with Some Micromechanical Models

The mode I and mode II of fracture toughness values obtained from finite element simulations are presented in Table 2.

Both the fracture toughness and the tensile strength of brittle foams depend on the fracture strength of the solid material [1]. In Figure 14a, the data for normalized fracture toughness of polyurethane foams for mode I, in comparison with the Gibson-Ashby model are shown. The fracture toughness is normalized with respect to fracture strength of polyurethane solid material, σ_{fs}, and to cell size, l, and plotted versus relative density, ρ^*/ρ_s. The solid line indicates the Gibson-Ashby model for open-cell foams, eqn (1), and has a slope of 1.5. A good agreement could be observed between the fracture toughness predicted based on the present study and the Gibson-Ashby micromechanical model.

Table 2. Mode I and mode II of fracture toughness results.

l (mm)	t (mm)	ρ^*/ρ_s [-]	$K_{IC,PUR}$ (MPa$\sqrt{m}$)	$K_{IIC,PUR}$ (MPa$\sqrt{m}$)
0.52	0.02	0.077	0.051	0.006
0.60	0.10	0.333	0.384	0.105
0.55	0.05	0.182	0.186	0.032
0.75	0.05	0.133	0.141	0.021
0.95	0.05	0.105	0.112	0.015

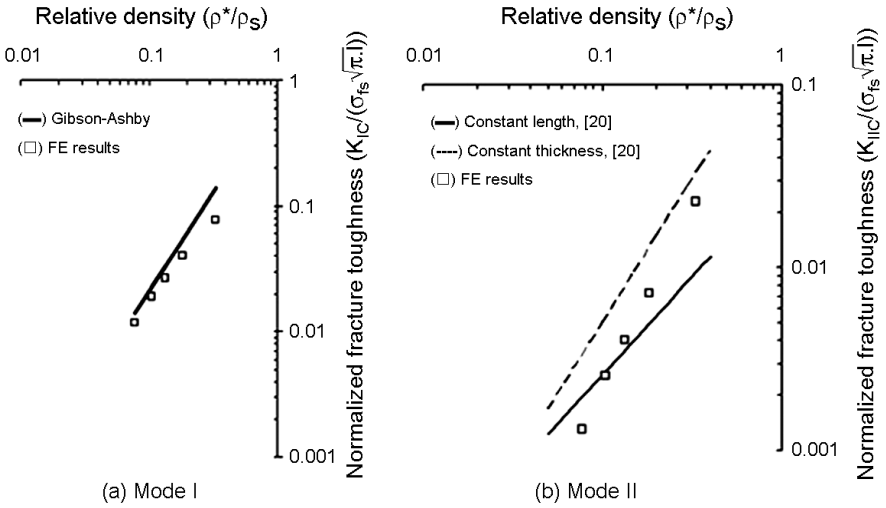

Figure 14. Normalized fracture toughness versus relative density: (a) mode I and (b) mode II.

Figure 14b presents the estimated mode II fracture toughness results, together with the micromechanical models of Choi et al. [20], eqns (2) and (3). It can be observed that the obtained results fall inside the limits drawn by the micromechanical models proposed by Choi et al. [20]. For values of $\rho^*/\rho_s < 0.1$, our results are smaller than those predicted by other micro-mechanical models [20].

Comparison with Experimental Data

Viana et al. [4] and Kabir et al. [25], used the procedure described by ASTM D5045 for determining the fracture toughness of poly(vinyl chloride) (PVC) and polyurethane (PUR) foams, respectively. They investigated the effect of density, specimen size, loading rate and cell orientation on fracture toughness. In the same line, Marsavina et al. [26] investigated the effect of density on fracture toughness of polyurethane foams. The results of the experimental fracture toughness [4,25,26] versus relative density are shown in Figure 15, together with the estimated FE values of fracture toughness. A good agreement can be observed and it thus validates our

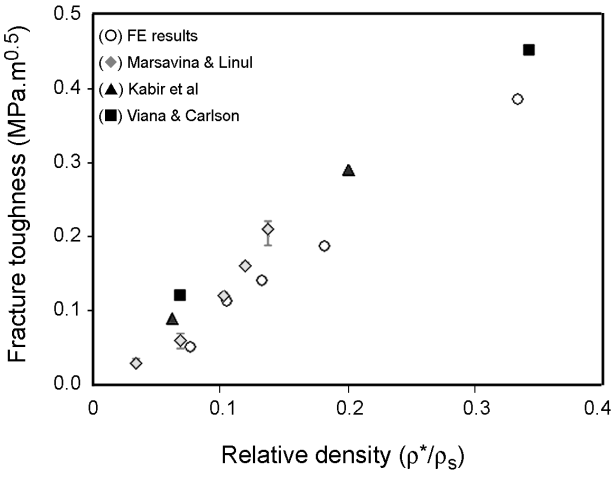

Figure 15. Comparison of estimated mode I fracture toughness by FE micromechanical model and experimental data.

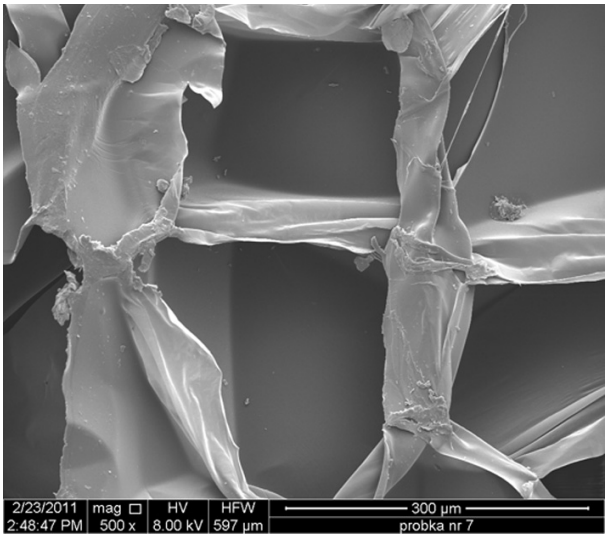

Figure 16. The cell microstructure of polyurethane foams used for experimental fracture toughness tests (relative density, $\rho^*/\rho_s = 0.034$).

predictions of fracture toughness based on the micromechanical finite element analysis.

Microstructural analysis was carried out for one of the tested foams. The initial cellular structure of rigid polyurethane foam with relative density, ρ^*/ρ_s = 0.034, used for experimental fracture toughness determination, is shown in Figure 16. It can be observed that the cell geometry is approximately rectangular, with a strut thickness of approximately 0.005 mm and a strut length between 0.275 to 0.3 mm.

CONCLUSION

Some concluding remarks can be drawn:

- A new 2D-solid micromechanical finite element model was proposed for predicting the fracture toughness of cellular polymers. The fracture toughness was predicted based on linear elastic fracture mechanics, by equating the maximum stress, $\sigma_{y,max}$, in the first unbroken strut with the fracture strength of solid material, σ_{fs}.

- The advantage of this model is that it fully describes the stress field in the solid struts. The stress distribution in the first un-cracked strut shows a complex stress (bending and tension) for mode I loading (Figure 9b), while for mode II loading a pure bending occurs (Figure 12b).

- The estimated fracture toughness was independent on crack length, indicating that the obtained values could be considered as a material related property.

- The estimated values for fracture toughness of polyurethane foams are in the range of 10^{-3}-10^{-1} MPa.m$^{0.5}$. Lower values were obtained for mode II fracture toughness (up to 10 times smaller than for mode I fracture toughness).

- The fracture toughness is strongly dependent on foam density.

- The comparison with other micromechanical models and experimental data of fracture toughness validates the micromechanical FE predictions presented in this paper.

- The real cell geometry of tested foams (Figure 16), is approximately the same with the modelled cell geometry (Figure 5).

ACKNOWLEDGEMENT

This work was partially supported by the strategic grant POSDRU6/1.5/S/13 (2008), of the Ministry of Labour, Family and Social Protection, Romania, co-financed by the European Social Fund - Investing in People.

REFERENCES

1. Gibson LJ, Ashby MF, *Cellular Solids, Structure and Properties*, Second Edition, Cambridge University, 26-234, 1997.
2. Beydokhti KK, Behravesh AH, Azdast T, An experiment study on mechanical and microstructural properties of microcellular foams of ABS composites, *Iran Polym J*, **15**, 555-567, 2006.
3. Grenestedt LJ, Effective elastic behavior of same models for 'perfect' cellular solids, *Int J Solid Struct*, **36**, 1471-1501, 1999.
4. Viana GM, Carlsson LA, Mechanical properties and fracture characterization of cross-linked PVC foams, *J Sandw Struct Mater*, **4**, 91-113, 2002.
5. Beverte I, Deformation of polypropylene foam Neopolen® P in compression, *J Cell Plast*, **40**, 191-204, 2004.
6. Esmaeilnezhad E, Rezaei M, Karim Razavi MK, The effect of alternative blowing agents on microstructure and mechanical characteristics of rigid polyurethane foam, *Iran Polym J*, **18**, 569-579, 2009.
7. Daxner T, Finite element modeling of cellular materials. In: *Cellular and Porous Materials in Structures and Processes*, Altenbach H, Ochsner A (Eds), Springer, 4-98, 2010.
8. Zhu HX, Knott JF, Mills NJ, Analysis of the elastic properties of open-cell foams with tetrakaidecahedral cells, *J Mech Phys Solid*, **45**, 319-325, 1997.
9. Bureau M, Kumar V, Fracture toughness of high density polycarbonate microcellular foams, *J Cell Plast*, **42**, 229-240, 2006.
10. Hawkins MC, O'Toole B, Jackowich D, Cell morphology and mechanical properties of rigid polyurethane foam, *J Cell Plast*, **41**, 267-285, 2005.

11. Ren XJ, Silberschmidt VV, Numerical modeling of low-density cellular materials, *Comp Mater Sci*, **43**, 65-74, 2008.
12. Mills NJ, *Polymer Foams Handbook: Engineering and Biomechanics Applications and Design Guide*, Elsevier, 12-173, 2007.
13. Fowlkes CW, Fracture toughness tests of a rigid polyurethane foam, *Int J Fracture*, **10**, 99-108, 1974.
14. McIntyre A, Anderton GE, Fracture properties of a rigid polyurethane foam over a range of densities, *Polymer*, **20**, 247-253, 1979.
15. Maiti K, Ashby MF, Gibson LJ, Fracture toughness of brittle cellular solids, *Scripta Metall Mater*, **18**, 213-217, 1984.
16. Brezny R, Green DJ, Fracture behavior of open-cell ceramics, *J Am Ceram Soc*, **72**, 1145-1152, 1989.
17. Huang JS, Gibson LJ, Fracture toughness of brittle foams, *Acta Metal Mater*, **39**, 1627-1636, 1991.
18. Green DJ, Fabrication and mechanical properties of light weight ceramics produced by sintering of hollow spheres, *J Am Ceram Soc*, **68**, 403-409, 1985.
19. Choi JB, Lakes RS, Fracture toughness of re-entrant foam material with a negative Poisson's ratio: experimental and analysis, *Int J Fracture*, **80**, 73-83, 1996.
20. Choi S, Sankar BV, A micromechanical method to predict the fracture toughness of cellular materials, *Int J Solid Struct*, **42**, 1797-1817, 2005.
21. Ableidinger A, Some aspects of the fracture behaviour of metal foams, PhD Thesis, Technische Universitat Wien, 2000.
22. Arakere NK, Knudsen EC, Wells D, McGill P, Swanson GR, Determination of mixed-mode stress intensity factors, fracture toughness, and crack turning angle for anisotropic foam material, *Int J Solid Struct*, **45**, 4936-4951, 2008.
23. Choi S, Sankar BV, Fracture toughness of carbon foam, *J Compos Mater*, **37**, 2101-2116, 2003.
24. Marsavina L, Fracture mechanics of foams. In: *Cellular and Porous Materials in Structures and Processes*, Altenbach H, Ochsner A (Eds), Springer, 1-46, 2010.
25. Kabir ME, Saha MC, Jeelani S, Tensile and fracture behavior of polymer foams, *Mater Sci Eng A-Struct*, **429**, 225-235, 2006.
26. Marsavina L, Linul E, Fracture toughness of polyurethane foams, experiments versus micro-mechanical models, *CD ROM Proc of 18th Eur Conf on Fracture, Dresden*, Germany, 30 Aug-3 Sep 2010.
27. Murakami Y, *Stress Intensity Factors Handbook*, Pergamon, Oxford, 931, 1987.